

On the Origin of a Band Gap in Compounds of Diamond-like Structures

Jürgen Köhler* and Shuiquan Deng

Max-Planck-Institut für Festkörperforschung, Heisenbergstrasse 1, D-70569 Stuttgart, Germany

Changhoon Lee and Myung-Hwan Whangbo*

Department of Chemistry, North Carolina State University, Raleigh, North Carolina 27695-8204

Received November 27, 2006

Electronic structure calculations were performed to examine the origin of a band gap present in most 18-electron half-Heusler compounds and its absence in NaTi. In these compounds of diamond-like structures, the presence or absence of a band gap is controlled by the σ antibonding between the valence s orbitals, and the bonding characteristics of the late-main-group elements depend on the extent of their *ns/np* hybridization. Implications of these observations on the formal oxidation state and the covalent bonding of the transition-metal atoms in 18-electron half-Heusler and related compounds were discussed.

Diamond and elemental Si are archetypal band-gapped compounds with a diamond lattice, and both compounds are considered to have strong covalent interactions between their adjacent tetrahedral sites through the sp^3 hybrid orbitals. These interactions lead to four bonding and four antibonding bands per two tetrahedral sites, and a band gap results with eight valence electrons per two sites. The diamond lattice of Tl^- anions in the Zintl compound NaTi is explained by supposing that the Tl^- ions with a $(ns)^2(np)^2$ configuration as in C and Si interact covalently. From this explanation and the fact that numerous Zintl compounds are insulators, one might be led to think that NaTi has a band gap, but NaTi is a regular metal.¹ The metallic versus insulating problem of diamond-like structures was first discussed by Kimball.² It should be mentioned that NaTi does not quite fit into the classification scheme of either intermetallic or ionic compounds in terms of ionic radii.³

Half-Heusler compounds AML consist of an electropositive atom A (e.g., Sc, Y), a late-transition-metal atom M (e.g., Ni, Pd, Au), and a heavy main-group atom L of the group 14 or 15 (e.g., As, Sn, Sb, Pb, Bi) and are structurally

closely related to NaTi. The atoms M and L form a zinc blende lattice (Figure 1a), which becomes a diamond lattice if $M = L$, and the atoms A occupy half the 10-coordinate sites made up of an M_4 tetrahedron and an L_6 octahedron (Figure 1b).

Most 18-electron half-Heusler (18eHH) compounds are regular semiconductors.⁴ The electronic structure of a 18eHH compound AML is described by the oxidation assignment $A^{n+}(ML)^{n-}$, where n is the number of valence electrons donated by A.^{4a,c} Qualitatively, the semiconducting property of most 18eHH compounds has been understood by noting that the 18-electron count around M implies a closed-shell electron configuration (i.e., $d^{10} + s^2 + p^6$).^{4a,c} In the present work, we probe the origin of a band gap in most 18eHH compounds and its absence in NaTi and discuss implications of our results, on the basis of first principles electronic band structure calculations^{5–7} for NaTi and representative 18eHH compounds ScAuSn,⁸ CaAuBi,⁹ and YAuPb.¹⁰

The band dispersion relations calculated for NaTi are presented in Figure 2a, where the valence s-orbital contributions of all of the atoms to the bands are indicated by the fat-band representation, and the corresponding density of states (DOS) plots in Figure 2b, where the Fermi level crosses

* To whom correspondence should be addressed. E-mail: j.koehler@fkf.mpg.de (J.K.), mike_whangbo@ncsu.edu (M.W.).

- (1) (a) Zintl, E.; Woltersdorf, G. *Z. Electrochem.* **1935**, *41*, 876. (b) Christensen, N. E. *Phys. Rev. B* **1985**, *32*, 207. (c) Schmidt, P. C. *Struct. Bonding* **1987**, *65*, 91.
- (2) Kimball, C. W. *J. Chem. Phys.* **1935**, *3*, 560.
- (3) Simon, A. *Angew. Chem.* **1983**, *95*, 194; *Angew. Chem., Int. Ed. Engl.* **1983**, *22*, 95.

- (4) (a) Jung, D.; Koo, H.-J.; Whangbo, M.-H. *J. Mol. Struct. (THEOCHEM)* **2000**, *527*, 113. (b) Galanakis, I.; Dederichs, P. H.; Papanikolaou, N. *Phys. Rev. B* **2002**, *66*, 134428. (c) Kandpal, H. C.; Felsner, C.; Seshadri, R. *J. Phys. D: Appl. Phys.* **2006**, *39*, 776.
- (5) In our density functional theory calculations, we employed the full-potential linearized augmented-plane-wave method embodied in the WIEN2k code 5 using the generalized gradient approximation of Perdew–Burke–Ernzerhof (ref 7). In all cases, the valence states were treated scalar relativistically, and no spin–orbit coupling was included. The muffin-tin radii used for all atoms were 2.5 Å. The cut-off angular momentum (l_{\max}) was 10 for the wave functions and 6 for the charge densities and potentials. The number of augmented plane waves included was about 356 per atom, i.e., $R_{MT}K_{\max} = 9$. The number of k points in the irreducible Brillouin zone used in the self-consistent calculations was 168.
- (6) See: <http://www.wien2k.at>.
- (7) Perdew, J. P.; Burke, S.; Ernzerhof, M. *Phys. Rev. Lett.* **1996**, *77*, 3865.
- (8) Eberz, U.; Seelentag, W.; Schuster, H.-U. *Z. Naturforsch.* **1980**, *B35*, 1341.
- (9) Iandelli, A. *Rev. Chim. Miner.* **1987**, *24*, 28.
- (10) Marazza, R.; Rossi, D.; Ferro, R. *J. Less-Common Met.* **1988**, *138*, 189.

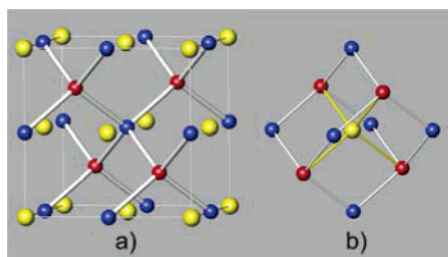


Figure 1. (a) Perspective view of the crystal structure of a half-Heusler compound AML ($A = \text{Ca}, \text{Sc}, \text{Y}$; $M = \text{Au}$; $L = \text{Sn}, \text{Sb}, \text{Pb}, \text{Bi}$). The yellow spheres represent the electropositive atoms A , the red spheres the transition-metal atoms M , and the blue spheres the main-group atoms L . (b) Perspective view of the coordinate environment of an electropositive atom A .

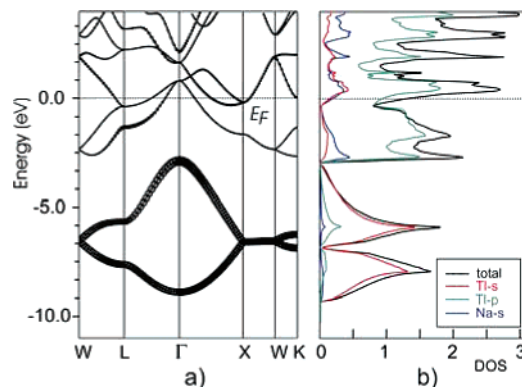


Figure 2. Calculated electronic structure of NaTi: (a) Dispersion relations of the bands around the Fermi level. (b) Total and partial DOS plots.

the three overlapping bands. The major orbital characters of the five-valence-electron bands containing eight electrons per $(\text{Ti}^-)_2$ (i.e., per primitive unit cell) vary, in ascending order, as follows: *the Ti 6s/Ti 6s σ -bonding band < the Ti 6s/Ti 6s σ -antibonding band < the three overlapping Ti 6p/Ti 6p σ -bonding bands <* Thus, with eight electrons per $(\text{Ti}^-)_2$, the Ti 6p bands are partially filled so that NaTi is a regular metal. Figure 2b exhibits a very weak 6s/6p hybridization, which is crucial for the absence of a band gap in NaTi. Extended Hückel tight-binding calculations¹¹ show that even the electronic structures of diamond and elemental Si become metallic if the valence ns orbitals (i.e., C 2s and Si 3s) are strongly contracted to prevent ns/np hybridization.

The band dispersion relations calculated for a representative 18eHH compound ScAuSn are presented in Figure 3a, where the Fermi level lies at the top of the three overlapping bands. The contributions of the Au 6s and Sn 5s orbitals are given with the fat-band representation and the corresponding DOS plots in Figure 3b–d. With 18 valence electrons filling the 9 valence bands completely, ScAuSn is a semiconductor with a small indirect band gap. The partial DOS plots of Figure 3b are consistent with the oxidation state 3+ for Sc and hence the electron-counting $[\text{AuSn}]^{3-}$. The Sn 5s and the Au 6s states are present between -8.0 and -10.0 eV and between -6.5 and 0.0 eV (Figure 3c,d), with stronger Sn 5s and Au 6s contributions in the lower and higher energy

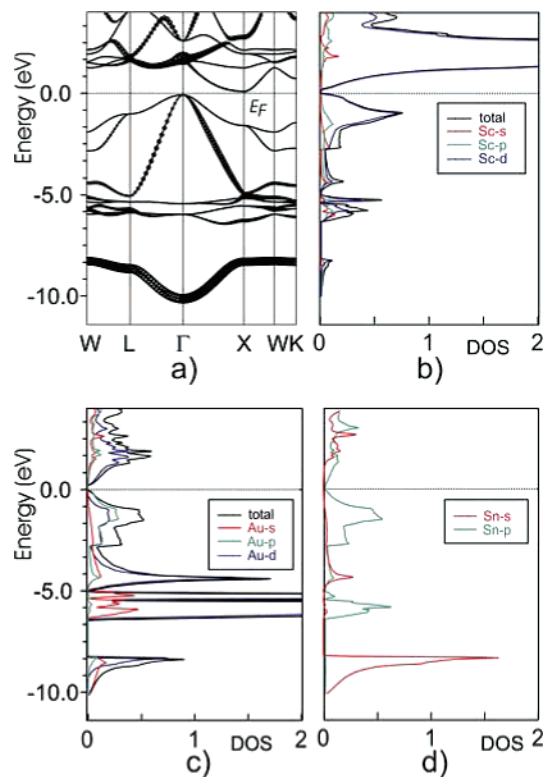


Figure 3. Calculated electronic structure of ScAuSn: (a) Dispersion relations of the bands around the Fermi level. (b) Total and partial DOS plots for Sc. (c) Partial DOS plots for Au. (d) Partial DOS plots for Sn.

regions, respectively. The Au 5d states occur primarily as sharp peaks between -6.5 and -5.0 eV, while the Au 6p states occur between -3.5 eV and 0.0 eV, where the Au 5d states are also present. The filled Sn 5p states occur where the filled Au 5d and filled Au 6p states are present (Figure 3c,d). According to these observations, the -8.0 to -10.0 eV region represents Sn 5s/Au 6s bonding and the -6.5 to -5.0 eV region primarily the Au 5d states with some Au 5d/Sn 5p bonding. The -3.5 to 0.0 eV region represents Au 5d,6p/Sn 5p bonding. This bonding analysis is supported by COHP calculations¹² carried out for the Au–Sn bond on the basis of first principles TB-LMTO¹³ calculations for ScAuSn (Figure S.1 in the Supporting Information).

The Sn 5s/Au 6s antibonding effect is not pronounced in the COHP plot in the -6.5 to 0.0 eV region because the latter overlaps with the regions of the Au 5d/Sn 5p bonding and the Au 5d,6p/Sn 5p bonding and because the bonding effects are stronger. Thus, the major orbital characters of the nine filled valence-electron bands of ScAuSn are described, in ascending order, as follows: *the wide Sn 5s/Au 6s σ -bonding band < the five narrow Au 5d bands < the wide Au 6s/Sn 5s σ -antibonding band < the two overlapping Au 6p/Sn 5p σ -bonding bands <* For simplicity, the Sn 5s/Au 6s σ -bonding and σ -antibonding bands will be referred to as the Sn 5s and Au 6s bands, respectively. It is crucial to note that the Au 6s band gradually

(11) (a) Whangbo, M.-H.; Hoffmann, R. *J. Am. Chem. Soc.* **1978**, *100*, 6093. (b) Our calculations were carried out by employing the CAESAR2 program package (Dai, D.; Ren, J.; Liang, W.; Whangbo, M.-H. <http://chvnmw.chem.ncsu.edu/>, 2002).

(12) Dronskowski, R.; Blöchl, P. *J. Phys. Chem.* **1993**, *97*, 8617.

(13) Tank, R.; Jepsen, O.; Burkhardt, A.; Andersen, O. K. TB-LMTO-ASA, version 4.7; MPI für Festkörperforschung: Stuttgart, Germany, 1998.

loses its s-orbital character as it approaches the Fermi level at Γ , where it gets only the Sn 5p- and Au 6p-orbital characters. At Γ , the Au 6s/Sn 5s σ -antibonding level lies above the Fermi level.

Except for the five narrow Au 5d bands, the filled valence-electron bands of ScAuSn are quite similar in general features to those of NaTi. However, the two compounds differ critically at the Γ point around the Fermi level: The energy levels of NaTi at Γ have the following sequence: *the Ti 6s/Ti 6s σ -bonding level < the Ti 6s/Ti 6s σ -antibonding level < the three degenerate Ti 6p/Ti 6p σ -bonding levels < ...* In contrast, the energy levels of ScAuSn at Γ have the following sequence: *the Au 6s/Sn 5s σ -bonding level of largely Sn 5s < the five Au 5d levels < the three degenerate Au 5d,6p/Sn 5p σ -bonding levels < the Au 6s/Sn 5s σ -antibonding level of largely Au 6s < ...* Namely, the most σ -antibonding level formed from the valence s orbitals lies lower in energy than the top of the σ -bonding bands formed from the valence p orbitals for NaTi (Figure 2a), but the opposite is the case for ScAuSn (Figure 3a). This means that the strongest σ -antibonding interaction between the Ti 6s orbitals is weaker than that between the Au 6s and Sn 5s orbitals, which is understandable because the Au–Sn bond of ScAuSn is considerably shorter than the Ti–Ti bond of NaTi (i.e., 2.780 vs 3.231 Å). The above observation implies that the σ -antibonding interactions between the valence s orbitals of M and L in AML can be enhanced by shortening the M–L bond, by increasing the diffuseness of the valence s orbitals of M and L, and by decreasing the energy difference between the valence s orbitals of M and L. If this σ -antibonding interaction is strong enough, an 18eHH compound might become a semiconductor with an indirect band gap rather than a regular metal. Our calculations predict CaAuBi¹⁴ to be a regular metal, although it is an 18eHH compound (Figure S.2a in the Supporting Information).¹⁵ However, YAuPb¹⁶ is predicted to be a semiconductor with nearly a zero band gap (Figure S.2b in the Supporting Information),¹⁵ as reported.^{4c} The most σ -antibonding level from the valence s orbitals of the M and L atoms lies below the top of the σ -bonding bands of the valence p orbitals in CaAuBi, but the opposite is the case in YAuPb because the Au–Bi bond is longer than the Au–Pb bond (i.e., 2.967 vs 2.914 Å), and the s-orbital energies of Bi, Pb, and Au increase in the order Bi 6s < Pb 6s < Au 6s.

Another important factor inducing a band gap in AML is the presence of low-lying d orbitals on the electropositive element A (e.g., Sc, Y). As shown in Figure 1b, each A is located at the center of an M₄ tetrahedron and an L₆ octahedron. In the σ -antibonding level at Γ , the valence ns orbitals of M are combined out of phase with those of L. As

a consequence, the ns orbitals of an M₄ tetrahedron form a group orbital of a₁ symmetry and those of an L₆ octahedron a group orbital of a_{1g} symmetry (Figure S.3 in the Supporting Information). Consequently, at Γ , the d orbitals of A do not interact with the σ -antibonding level of the ns orbitals. However, these d orbitals interact with the triply degenerate level of the np valence orbitals. This causes a preferential lowering of the triply degenerate level, hence leading to a band gap. Such a preferential lowering does not occur when the element A does not have low-lying d orbitals (e.g., Ca), thereby leading to partially filled bands as found for CaAuBi (Figure S.2a in the Supporting Information).

All five Au 5d block bands of ScAuSn are completely filled (Figure 3c), hence leading to the d-electron count of 5d,¹⁰ and lie well below the Fermi level so that the 10 d electrons of Au may be regarded as “pseudocore” electrons. Then, the 18-electron rule is reduced to the octet rule for ScAuSn, and each Au atom may be regarded as a “pseudo”-main-group element with eight valence electrons to form four polar covalent Au–Sn bonds. Thus, the covalent electron counting¹⁷ leads to four electrons in the 6s and 6p orbitals for each Au and hence to the s- and p-electron counts of 6s²6p² because the Au 6s bands are completely filled. As a result, each Au of ScAuSn has the electron configuration (5d)¹⁰(6s)²(6p)². In terms of the ionic electron counting,¹⁷ this configuration is equivalent to a formal Au³⁺ ion so that the oxidation assignment of (Sc³⁺)(Au³⁺)(Sn⁰) is appropriate for ScAuSn. Formal negative transition-metal ions found in compounds of late-transition-metal atoms with late-main-group elements of typically the fifth and sixth periods,^{18–20} which include 18eHH compounds, have strong covalent interactions with their surrounding main-group elements. The presence of such transition-metal anions is manifested by the fact that the frontier orbitals of these compounds are not described by the transition-metal nd orbitals but by the transition-metal (n+1)p orbitals.

Acknowledgment. The work at North Carolina State University was supported by the Office of Basic Energy Sciences, Division of Materials Sciences, U.S. Department of Energy, under Grant DE-FG02-86ER45259.

Supporting Information Available: Figures S.1–S.3. This material is available free of charge via the Internet at <http://pubs.acs.org>.

IC062256X

(14) Merlo, F.; Pani, M.; Fornasini, M. L. *J. Less-Common Met.* **1990**, *166*, 319.

(15) See the Supporting Information.

(16) Marazza, R.; Rossi, D.; Ferro, R. *J. Less-Common Met.* **1988**, *138*, 189.

(17) For further discussions of the covalent, ionic, and modified electron-counting schemes, see: (a) Lee, K.-S.; Koo, H.-J.; Dai, D.; Ren, J.; Whangbo, M.-H. *Inorg. Chem.* **1999**, *38*, 340. (b) Lee, K.-S.; Koo, H.-J.; Dai, D.; Ren, J.; Whangbo, M.-H. *J. Solid State Chem.* **1999**, *147*, 11.

(18) (a) Köhler, J.; Chang, J.-H. *Angew. Chem., Int. Ed. Engl.* **2000**, *39*, 1998. (b) Köhler, J.; Chang, J.-H.; Whangbo, M.-H. *J. Am. Chem. Soc.* **2005**, *127*, 2277.

(19) Sevov, S. C.; Corbett, J. D. *J. Am. Chem. Soc.* **1993**, *115*, 9089.

(20) Whangbo, M.-H.; Lee, C.; Köhler, J. *Angew. Chem., Int. Ed.* **2006**, *45*, 7465.